Stable trimerization of recombinant rabies virus glycoprotein ectodomain is required for interaction with the p75^{NTR} receptor

Ludmilla Sissoëff,[1]† Mohamed Mousli,[1]†‡ Patrick England[2] and Christine Tuffereau[1]

[1]Laboratoire de Virologie Moléculaire et Structurale, UMR 2472 CNRS-INRA, 91198 Gif-sur-Yvette, France

[2]Plateforme de Biophysique des Macromolécules et de leurs Interactions, Institut Pasteur, 75015 Paris, France

Correspondence
Christine Tuffereau
christine.tuffereau@vms.cnrs-gif.fr

Native rabies virus glycoprotein (RVGvir) is a trimeric, membrane-anchored protein that has been shown to interact with the p75^{NTR} neurotrophin receptor. In order to determine if the RVG trimeric oligomerization state is required for its binding with p75^{NTR}, different soluble recombinant molecules containing the entire RVG ectodomain (RVGect) were expressed alone or fused at its C terminus to the trimerization domain of the bacteriophage T4 fibritin, termed 'foldon'. The oligomerization status of recombinant RVG was investigated using sedimentation in sucrose gradient and p75^{NTR} binding assays. It was found that, in the absence of the fibritin foldon, recombinant RVGect forms unstable trimers that dissociate into monomers in a concentration-dependent manner. C-terminal fusion with the foldon induces stable RVG trimerization, which is concentration-independent. Furthermore, the fibritin foldon maintains the native antigenic structure of the carboxy part of RVGect. Cell binding experiments showed that RVG trimerization is required for efficient interaction with p75^{NTR}. However, the exact mode of trimerization appears unimportant, as trimeric recombinant RVGect (fused to the fibritin foldon) and RVGvir both recognize p75^{NTR} with similar nanomolar affinities, as shown by surface plasmon resonance experiments. Altogether, these results show that the C-terminal fusion of the RVG ectodomain with the fibritin foldon is a powerful way to obtain a recombinant trimeric native-like structure of the p75^{NTR} binding domain of RVG.

Received 25 March 2005
Accepted 13 May 2005

INTRODUCTION

Rabies virus (RV) is a non-segmented, negative-strand RNA virus belonging to the genus *Lyssavirus* of the family *Rhabdoviridae*. It is highly neurotropic and can cause fatal encephalomyelitis in mammals (Warrell & Warrell, 2004). Its envelope contains a single type I glycoprotein G (RVG) of 65 kDa organized as a trimer in the membrane context (Whitt *et al.*, 1991; Gaudin *et al.*, 1992). RVG plays a major role during viral entry: it is responsible for the binding of the virus to the target cells and for the fusion between viral and cell membranes during the endocytosis of the virus. RVG is also the main viral antigen and induces both humoral and cellular immune responses. Its antigenic structure has been extensively investigated (Cox *et al.*, 1977). Two major antigenic sites (sites II and III), one minor site (site 'a') and several epitopes have been described (Lafon *et al.*, 1983; Seif *et al.*, 1985; Prehaud *et al.*, 1988; Dietzschold *et al.*, 1990; Benmansour *et al.*, 1991; Lafay *et al.*, 1996). Specific interactions between RVG and neuronal cell surface molecules have been demonstrated (Tuffereau *et al.*, 1998a), suggesting the existence of specific neuronal receptor(s). Several candidates have been proposed so far: the nicotinic acetylcholine receptor (nACh) (Lentz *et al.*, 1983), the neural cell adhesion molecule (NCAM) (Thoulouze *et al.*, 1998) and the neurotrophin receptor (p75^{NTR}) (Tuffereau *et al.*, 1998b). In our laboratory, an expression cloning approach using soluble RVG to screen a neuroblastoma cell library led us to the identification of the murine p75^{NTR} as a candidate RVG receptor (Tuffereau *et al.*, 1998b). Direct interactions between RVG and p75^{NTR} have been demonstrated (Langevin *et al.*, 2002) and the binding domains have been identified on both molecules. The p75^{NTR} binding domain of RVG has been mapped more precisely through the characterization of viral mutants resistant to the neutralization by a soluble form of

†These authors contributed equally to this work.

‡Present address: Laboratoire Immuno-Biotechnologie, Institut Pasteur de Tunis, 1002 Tunis-Belvédère, Tunisia.

A supplementary table showing primers used in the construction of recombinant RVG clones is available as supplementary material in JGV Online.

the receptor: it is located on both sides of antigenic sites III and 'a' (Langevin & Tuffereau, 2002).

$p75^{NTR}$ expression in the adult is essentially restricted to the peripheral and the central nervous systems. $p75^{NTR}$ contains four cysteine-rich domains (CRD1 to CRD4) in its N-terminal ectodomain and a type II death domain (Liepinsh *et al.*, 1997) in its cytoplasmic C-terminal segment, both features characteristic of the tumour necrosis factor (TNF) receptor superfamily (Locksley *et al.*, 2001). However, the neurotrophins (NGF, BDNF, NT3 and NT4), which are the natural ligands of $p75^{NTR}$, differ from most ligands of the TNF receptor family by their oligomerization state, neurotrophins being dimers (McDonald *et al.*, 1991), while TNF-type ligands are trimers (Park *et al.*, 1999). Neurotrophins bind to $p75^{NTR}$ with nanomolar range affinities, and their binding site has been mapped to a region encompassing both CRD2 and CRD3 (Welcher *et al.*, 1991; Yan & Chao, 1991; Baldwin & Shooter, 1995). The three-dimensional structure of the $p75^{NTR}$–NGF complex has recently been solved and shows an asymmetric complex consisting of one $p75^{NTR}$ molecule interacting with the NGF dimer (He & Garcia, 2004). In our laboratory, we have demonstrated that RVG is a new $p75^{NTR}$ ligand, which differs from the neurotrophins in several features (Langevin *et al.*, 2002). Like TNF, it is a specific trimeric ligand and it binds to the first CRD of $p75^{NTR}$ with a very high affinity ($K_d = 30$ pM). As expected from the different localization of the binding sites on $p75^{NTR}$, no competition was observed between RVG and NGF.

A stable trimeric organization seems to be required for the ligands of TNF receptors to induce their physiological effect, as reported recently for two of them: Fas ligand (Shiraishi *et al.*, 2004) and TRAIL (Kim *et al.*, 2004). We therefore questioned if, in a similar way, RVG trimerization is required for its interaction with $p75^{NTR}$. Although native RVG extracted from virions with detergent is isolated as a stable trimer (Gaudin *et al.*, 1992), recombinant RVG ectodomains have been reported to be secreted as monomers (Gaudin *et al.*, 1999) or unstable trimers (Wojczyk *et al.*, 1995, 1998). The antigenic structure strongly differs between the trimeric and monomeric RVGs (Gaudin *et al.*, 1999; Maillard & Gaudin, 2002). It has been demonstrated that stable trimerization of RVG requires the presence of a hydrophobic amino acid-rich sequence (not necessarily the native transmembrane domain). Besides the transmembrane domain, the C-terminal part of the RVG ectodomain also plays a role in its trimerization (Maillard & Gaudin, 2002).

Several exogenous oligomerization motifs have been successfully used to promote stable trimers of soluble recombinant proteins: the GCN4 leucine zipper (Harbury *et al.*, 1993), the trimerization motif from the lung surfactant protein (Hoppe *et al.*, 1994), collagen (McAlinden *et al.*, 2003) and the phage T4 fibritin 'foldon' (Miroshnikov *et al.*, 1998). The fibritin foldon, a 27 aa sequence, adopts a β-propeller conformation (Tao *et al.*, 1997), and can fold and trimerize in an autonomous way (Letarov *et al.*, 1999). It has been reported recently that this foldon can successfully induce stable trimerization of other fibrous motifs such as phage T4 short-tail fibres (Miroshnikov *et al.*, 1998) and adenovirus fibres (Krasnykh *et al.*, 2001; Papanikolopoulou *et al.*, 2004a), as well as a viral human immunodeficiency virus glycoprotein, gp140 (Yang *et al.*, 2002).

In this study, we have expressed in insect cells, using a recombinant baculovirus, the full-length recombinant RVG ectodomain (aa 1–439) from the Pasteur virus (PV) strain, with or without the fibritin foldon fused at its C terminus. We have characterized its oligomeric and antigenic structure. We have also determined if its ability to interact with $p75^{NTR}$, either membrane-anchored or soluble, was dependent on its oligomerization state. Then, we performed surface plasmon resonance experiments to determine the binding parameters of recombinant RVG in comparison to those of native RVG extracted from virions.

METHODS

Cells and viral glycoprotein. Cos7 and BHK-21-BSR cells were grown at 37 °C in Dulbecco's modified Eagle's medium (DMEM; Invitrogen) supplemented with 10 % fetal calf serum (FCS) in a 5 % CO_2 humidified incubator.

Sf21 insect-cells from *Spodoptera frugiperda* (Invitrogen) were grown at 28 °C in TC100 medium (Invitrogen) supplemented with 10 % FCS.

Native viral glycoprotein (RVGvir) from purified virions was detergent extracted and purified using a protocol previously described by Gaudin *et al.* (1992).

Antibodies and plasmids. We used neutralizing anti-glycoprotein monoclonal antibodies (mAbs) prepared and characterized in our laboratory (Benmansour *et al.*, 1991; Raux *et al.*, 1995; Lafay *et al.*, 1996; Maillard & Gaudin, 2002). mAb 27DD5 binds to RVG antigenic site II, 6B1 to site III, 9B4 and 40EB1 to the minor site 'a' and 1D1 binds to a linear epitope located between aa 255 and 276. Two non-neutralizing antibodies were also used: 17D2 binds to the same linear epitope as 1D1, and 21H8 to an unknown epitope present on both monomeric and trimeric RVG (Maillard & Gaudin, 2002). mAb D1 (directed against site III and specific of the trimeric state) (Jallet *et al.*, 1999; Desmezieres *et al.*, 2003) and the rabbit polyclonal anti-RVG antibody were kindly given by Pierre Perrin and Noël Tordo (Institut Pasteur, Paris, France). The mouse polyclonal anti-fibritin antibody was kindly provided by Dr Mezyanzhinov (Institute of Bioorganic Chemistry, Moscow, Russia). The bacteriophage T4 fibritin plasmid (pT412w13) was provided by A. Letarov (S.N. Winogradsky Institute of Microbiology, Moscow, Russia). The human $p75^{NTR}$ plasmid was donated by Barbara Hempstead (Cornell University, New York, USA). The mouse mAb ME20.4 (ATCC) was used for the detection of $p75^{NTR}$.

RVG constructs and production of recombinant baculoviruses. Plasmids were constructed by insertion of PCR-amplified RVG fragments into the PVL1393 insect cell expression system (Pharmingen). Recombinant plasmids based on PVL1393 and expressing RVGect, RVGect-Fib and RVG-G_8-Fib of the PV RV strain were constructed as follows: the fragment encoding the RVG ectodomain comprising residues 1–439 was amplified by PCR with *Pfu* polymerase (Boehringer) using pairs of primers as described

in Supplementary Table S1 and the pcDNA1G vector as template (Gaudin *et al.*, 1999). Similarly, the fibritin foldon was amplified using the pT412w13 plasmid as template and specific pairs of primers. PCR-amplified DNA fragments were digested using appropriate restriction enzymes and cloned into the linearized PVL1393 vector. These recombinant plasmids were used for co-transfection of Sf21 cells with linearized *lacZ* baculovirus DNA from the *Autographa californica* nuclear polyhedrosis virus as previously described (Tuffereau *et al.*, 1998a).

Production of soluble recombinant RVGs. Monolayers of Sf21 cells were infected with different G-expressing recombinant baculoviruses at an m.o.i. of 3–10 p.f.u. per cell in TC100 medium containing 2 % fetal bovine serum. Two days after infection, the supernatants were collected and clarified at 3000 ***g*** for 10 min in a GDK Beckman centrifuge before further processing.

For surface plasmon resonance analysis and sedimentation gradient analysis, a 10-fold concentration of the supernatant was performed using Vivaspin 30 (Vivascience) concentrators.

Production of soluble recombinant human p75^{NTR}. The human p75^{NTR} cDNA sequence (containing aa 1–168) was PCR amplified using primers 5′-GCGGATCCAAAGGAGGCATGCCCC-3′ and 5′-CGCGGATCAGTGGTGGTGGTGGTGGTGAATCCAA-CGGCCAGGGAT-3′, and cloned into the pVTBac vector (provided by D. Tessier, CNRC, Montréal, Canada) digested by *Bam*HI. The pVTBac plasmid encodes the mellitin signal peptide, allowing efficient secretion of p75^{NTR}. To produce p75^{NTR}–His$_6$, Sf21 cells were infected by the recombinant baculoviruses (m.o.i. of 3) in serum-free medium (SF900; Invitrogen). Three days post-infection, the medium was collected and clarified by centrifugation at 3000 ***g*** for 15 min. The supernatant was extensively dialysed against 50 mM Tris buffer (pH 8) at 4 °C and was then incubated overnight with Ni-NTA resin (Qiagen). The resin was washed once with 20 mM imidazole in 300 mM NaCl, 10 mM Tris (pH 8) buffer; bound proteins were eluted with 100 mM imidazole in the same buffer. The p75^{NTR}-containing fractions were pooled, concentrated and then dialysed against PBS.

Immunoprecipitations. Supernatants (250 µl) from Sf21-infected cells were incubated with 2 µl of several anti-RVG mAbs for 2 h at 4 °C. Protein A–Sepharose (Sigma) was then added and the mixture was incubated for 1 h at 4 °C. The resulting immune complexes were centrifuged and washed twice with Tris buffer (25 mM Tris/HCl pH 7·5, 137 mM NaCl, 0·7 mM Na_2HPO_4, 5 mM KCl) containing 1 % CHAPS and 2 % cocktail inhibitors from Sigma (0·1 mg chymostatin ml^{-1}, 0·1 mg antipain ml^{-1}, 0·1 mg leupeptin ml^{-1}, 0·1 mg pepstatin ml^{-1} and 0·2 mg aprotinin ml^{-1}). The complexes were then boiled for 5 min in Laemmli buffer and analysed by Western blot using a polyclonal rabbit anti-RVG antibody.

Sucrose gradient analysis. An aliquot (200 µl) of supernatants from Sf21-infected cells was loaded on linear sucrose gradients. Gradients were prepared from stocks of 5 and 20 % (w/v) sucrose in Tris buffer. The gradients were then centrifuged at 32 000 r.p.m. for 16 h at 4 °C using a SW41 rotor (Beckman). Fractions (12 × 1 ml) were collected from the bottom of each gradient. The pellet was resuspended in 1 ml Tris buffer. Each fraction (15 µl) was analysed by Western blot using the anti-RVG mAb 17D2.

SDS-PAGE and immunoblotting analysis. Proteins present in the supernatant of infected Sf21 cells were denatured in Laemmli buffer with or without heating at 95 °C for 5 min. Electrophoresis was then carried out in a discontinuous 12 % SDS-PAGE gel. Proteins were transferred onto nitrocellulose membranes (BA85; Schleicher & Schuell). Membranes were saturated with 5 % skimmed milk in Tris-buffered saline (TBS) (50 mM Tris/HCl pH 8, 150 mM NaCl) containing 0·05 % Tween 20 for 30 min and then incubated overnight with appropriate anti-RVG or anti-fibritin antibodies. Membranes were washed three times in TBS/Tween and incubated for 2 h with a peroxidase-conjugated secondary antibody (Sigma) diluted 1 : 3000. RVG was then detected after extensive washing in TBS/Tween by enhanced chemiluminescence (ECL) Western blotting detection reagent (Amersham Biosciences). Quantification of the signal intensity was performed by comparative densitometry, using the NIH Image software.

Evaluation of the binding of RVG using the *β*-galactosidase assay. Transfected Cos7 cells with p75^{NTR} were incubated with 2 ml of supernatant from insect cells expressing the different recombinant RVG proteins and RVG binding was detected as previously described (Langevin *et al.*, 2002). X-Gal (5-bromo-4-chloro-3-indolyl-*β*-D-galactopyranoside; Gerbu) was used as a substrate for immunostaining (Tuffereau *et al.*, 1998b) and ONPG (*O*-nitrophenyl-*β*-D-galactopyranoside; Sigma) for colorimetric assays. Cells were incubated in presence of 0·66 mg ONPG ml^{-1} in 60 mM $Na_2HPO_4.7H_2O$, 40 mM $NaH_2PO_4.2H_2O$, 10 mM KCl, 1 mM $MgSO_4.7H_2O$, pH 7 for 30 min at 37 °C prior to reading the absorbance at 410 nm. Background (values obtained in the absence of RVG) was substracted for each dilution.

Determination of the active concentration of the protein preparations. p75^{NTR} was covalently linked, through its solvent-accessible primary amine groups, to the carboxymethylated dextran matrix of a CM5 sensorchip, using a Biacore 2000 apparatus and the Amine Coupling kit (Biacore): a density of 10 650 resonance units (RU; approx. 10 ng mm^{-2}) was thus attained. The active concentrations of recombinant RVGs were determined under conditions of partial mass transport limitation as previously described (Zeder-Lutz *et al.*, 1999). Briefly, two dilutions of each preparation were injected for 5 min across the CM5(p75) surface at seven different flow rates ranging from 2 to 100 µl min^{-1}. Control experiments were performed on an empty CM5 surface. The active concentrations were determined by analysing the initial binding rates with the BIA-CONC program.

Determination of the kinetic parameters of the interaction between p75^{NTR} and RVG. All the assays were performed on a Biacore 2000 instrument equilibrated at 25 °C with PBS pH 6·2, at a flow rate of 20 µl min^{-1}. Seven thousand RU of the Penta-His mAb (Qiagen) were covalently immobilized on a CM5 sensorchip, using the Amine Coupling kit. Recombinant His$_6$-tagged p75^{NTR} (p75^{NTR}–His$_6$) was captured to a level of 250 RU on the anti-His$_6$ surface. Ten different concentrations of soluble recombinant RVGect-G$_8$-Fib supernatant, as well as 10 concentrations of native RVGvir, were then injected across the anti-His$_6$/p75^{NTR}–His$_6$ surface for 10 min, and the dissociation of the complexes was followed for a further 10 min. Control experiments were performed by injecting RVG preparations directly onto the anti-His$_6$ surface. The association and dissociation profiles were analysed with a non-linear least squares algorithm implemented in the BIAevaluation 3.2 software (Biacore), using single-exponential functions of time.

RESULTS

Soluble recombinant RVGs are expressed in insect cells

Three different RVG constructs from the PV RV strain, all of them retaining the original RVG signal peptide, were designed (Fig. 1a). The first one (RVGect), containing the entire ectodomain (439 aa), is identical to the one that has been expressed previously in mammalian cells (Gaudin *et al.*, 1999). The other two, RVGect-Fib and RVGect-G$_8$-Fib, were

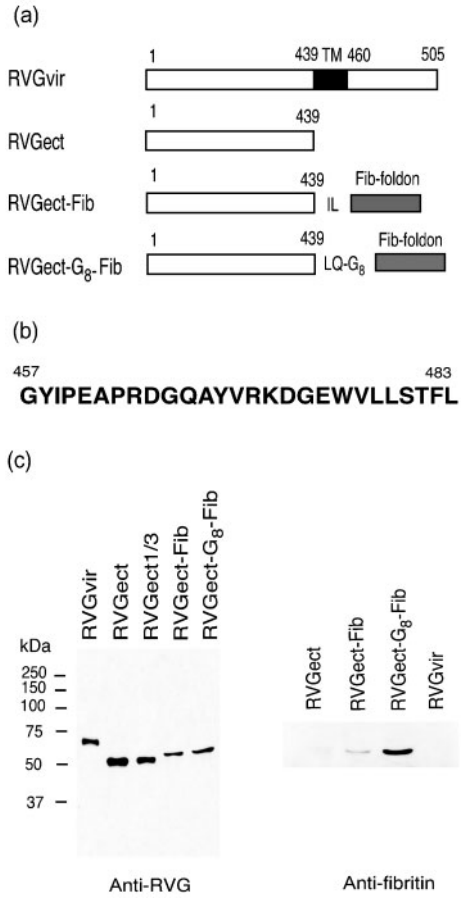

Fig. 1. Expression of recombinant RVGs in insect cells. (a) Schematic representation of the different RVGs used in this study: RVGvir, full-length RVG extracted from the virus; RVGect, RVG ectodomain (residues 1–439); RVGect-Fib and RVGect-G_8-Fib, fusion proteins with the fibritin 'foldon' at the C-terminal end of the RVG ectodomain, directly fused or linked through a sequence of eight glycines. Two extra amino acids [(I and L) and (L and Q)] were introduced, respectively, as a result of the cloning strategy. (b) Amino acid sequence of the bacteriophage T4 fibritin 'foldon' (residues 457–483). (c) Immunodetection of the recombinant RVGs expressed in insect cells detected by Western blotting using an anti-RVG mAb (17D2) (left panel) or a mouse polyclonal anti-fibritin antibody (right panel). Lane RVGvir: 70 ng of trimeric RVGvir. Lanes RVGect, RVGect-Fib and RVGect-G_8-Fib: 15 μl of cell supernatant. Lane RVGect 1/3: 5 μl of cell supernatant.

fused with a trimerization domain (Fig. 1b) (namely the fibritin foldon from the bacteriophage T4) at their C-terminal extremity. For RVGect-G_8-Fib, a linker consisting of eight glycine residues was introduced between the RVG coding sequence and the fibritin foldon in order to avoid steric hindrance and conformational interference.

First, we investigated if the different RVGs were secreted in the supernatant of Sf21 cells infected with the corresponding recombinant baculoviruses (Fig. 1c). The different RVGs migrated on SDS-PAGE according to their predicted molecular masses: about 50 kDa for RVGect and 55 kDa for the chimeric RVGs. The presence of the fibritin foldon in the chimeric proteins was demonstrated by Western blot analysis using a polyclonal anti-fibritin antibody (Fig. 1c). Quantification of the amount of secreted recombinant RVGs was done by comparison with a known amount of purified full-length RVGvir run on the same gel, and quantification of the bands on the Western blot was performed using the NIH Image analysis software. The mean concentration of RVGect was 5–10 μg ml^{-1}. The presence of the foldon at the C terminus of the RVG induces a significant reduction of the secretion of the chimeric molecules, and the amount of RVGect-Fib and RVGect-G_8-Fib produced was three to five times lower than that of RVGect.

Several attempts to immuno-purify recombinant RVG yielded inactive proteins owing to the harsh elution conditions, thus all the following analyses were performed on clarified cell supernatants.

Fibritin foldon stabilizes RVG oligomeric and antigenic structure

We investigated the oligomeric state of recombinant RVGs by analysing their sedimentation properties on a sucrose gradient (Fig. 2). While RVGect sedimented in fractions 10–12, corresponding to the sedimentation of a monomer, recombinant RVGect-Fib and RVGect-G_8-Fib were detected in fractions 8 and 9 or 6 to 10, respectively. Trimeric virus-extracted native RVG migrated in fractions 5–10. These results show that chimeric RVG containing

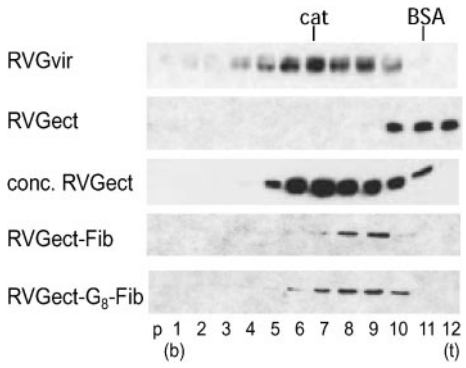

Fig. 2. Analysis of recombinant RVGs by ultracentrifugation on a 5–20 % sucrose gradient. Supernatants from Sf21 cells infected with recombinant RVG baculoviruses were deposited on a 5–20 % (w/v) sucrose gradient and ultracentrifuged. For RVGect, a 10-fold concentrated supernatant (conc. RVGect) was also analysed. Trimeric RVGvir was analysed in the same way on a gradient containing 1 % CHAPS. After centrifugation, 1 ml fractions (1–12) were collected and analysed by Western blotting using the anti-RVG mAb 17D2. (b) and (t) indicate the bottom and the top of the gradient, respectively, and p the pellet. The positions of the standards, catalase (cat) and BSA, corresponding to trimers and monomers, respectively, are indicated.

the fibritin foldon sediments as trimers. Using cross-linking experiments, the existence of trimers and oligomers was detected for all recombinant RVGs (data not shown). Altogether, these results suggest that, in the absence of fibritin, RVGect oligomers are dissociated in the sucrose gradient and that the fibritin foldon stabilizes the oligomeric structure of RVG. When the supernatant containing RVGect was concentrated 10-fold, it was also found in fractions 5–11 (Fig. 2), as RVGvir, showing that the proportion of trimer increases with the concentration of the RVGect samples. When this supernatant was diluted to its initial concentration, RVGect was found again in fractions 10–12 (data not shown). Altogether, this confirms the existence of a reversible and concentration-dependent trimer/monomer equilibrium.

C-terminal fusion of the fibritin foldon has been reported to confer resistance to SDS denaturation for chimeric molecules (Krasnykh *et al.*, 2001). We therefore analysed the SDS susceptibility of recombinant RVGs, by loading them on to an SDS-PAGE gel, either directly or after boiling for 5 min (Fig. 3). RVGect-G_8-Fib migrated principally as a high molecular species (Fig. 3a), probably corresponding to partially unfolded intermediates (I), in which RVG is denatured while the fibritin trimer is maintained. Similar unfolded intermediates have previously been reported for adenovirus fibre (Mitraki *et al.*, 1999). The fibritin trimers only dissociate when boiled (Fig. 3b). In contrast, RVGect and RVGect-Fib migrated as monomers in the presence or absence of heat denaturation; however, when electrophoresis was performed at 4 °C, some trimers and oligomers could also be detected for RVGect-Fib (data not shown). These results show that RVGect forms unstable trimers and that the fibritin foldon stabilizes the oligomer. Since the oligomeric stability of RVGect-G_8-Fib is greater than that

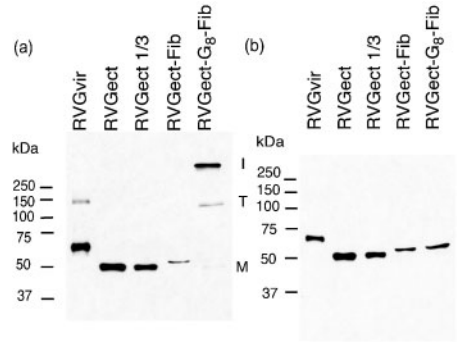

Fig. 3. Sensitivity of RVG oligomers to heat denaturation. Supernatants from Sf21 cells infected with recombinant RVG baculoviruses or RVGvir were denatured with Laemmli buffer and loaded on to a 10 % SDS gel without (a) or with (b) prior treatment at 95 °C. RVG was visualized by Western blotting with the anti-RVG mAb 17D2. M, Monomer; T, trimer; I, unfolded intermediates.

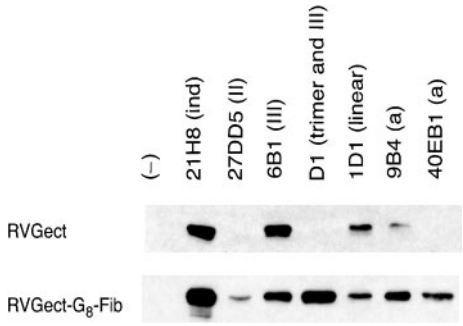

Fig. 4. Antigenic structure of the recombinant RVGs: RVGect and RVGect-G_8-Fib. Recombinant RVGs were immunoprecipitated with anti-RVG mAbs. Immune complexes were analysed by Western blotting using a rabbit polyclonal anti-RVG antibody. The antibody specificities are as follows: 27DD5, site II; 1D1, linear epitope; 6B1 and D1, site III; D1, trimer interface; 9B4 and 40EB1, site 'a'; and 21H8 (ind), conformation-independent.

of RVGect-Fib, we focused hereafter on the functional characterization of RVGect-G_8-Fib.

We thus compared the antigenic structure of RVGect and RVGect-G_8-Fib by immunoprecipitation (Fig. 4). While RVGect was only efficiently recognized by two mAbs (21H8 and the site III-specific 6B1), RVGect-G_8-Fib was immunoprecipitated well by all the mAbs with the exception of 27DD5 (site II-specific). Interestingly, a drastic difference was observed with a site III- and trimer-specific antibody (D1), which immunoprecipitated only RVGect-G_8-Fib but not RVGect. We also noticed a better recognition of RVGect-G_8-Fib by antibodies recognizing specifically site 'a' (9B4 and 40EB1).

These results show that the fibritin foldon stabilizes not only the RVG oligomeric structure, but also its antigenic structure, at least in its C-terminal region, since the antigenic site III and the site 'a' are located between aa 330 and 343.

RVG trimerization is required for p75^{NTR} interaction

We then investigated the ability of recombinant RVGs to interact with p75^{NTR}, either membrane-anchored or soluble. Supernatants from insect cells infected with the different recombinant baculoviruses, containing the same amount of RVG, were incubated with Cos7 cells transiently transfected with p75^{NTR}. RVG binding to p75^{NTR}-expressing cells was demonstrated by immunostaining.

A strong specific staining of transfected cells was observed with the recombinant RVGect-G_8-Fib (Fig. 5a), while that observed with the recombinant RVGect was much weaker. No RVGect-G_8-Fib binding was observed for untransfected cells. Similar experiments were performed with different RVG dilutions and quantified using a colorimetric assay

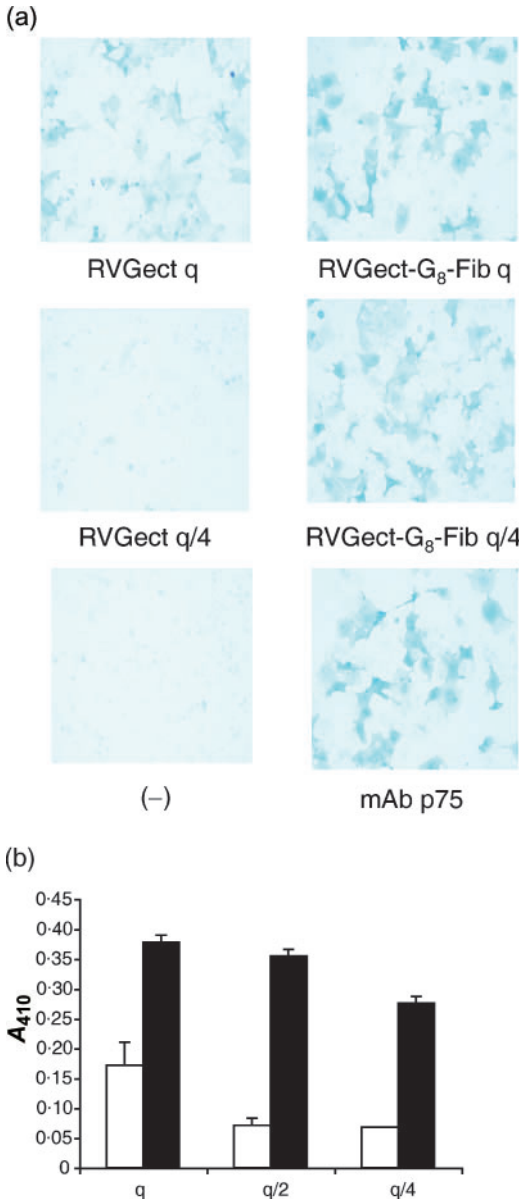

Fig. 5. Interaction of recombinant RVGs with Cos7 cells expressing $p75^{NTR}$. Supernatants from infected Sf21 cells containing the same amount (q) of RVGect and RVGect-G_8-Fib were diluted (q/2 and q/4) and incubated with Cos7 cells, transiently transfected by $p75^{NTR}$, followed by the anti-RVG mAb 21H8 immunostaining (a). Negative control, binding of RVGect-G8-Fib on untransfected cells (–); positive control, cells stained by a mAb anti-$p75^{NTR}$, are included. (b) Colorimetric assay. Each normalized bar represents the mean of three determinations, for RVGect (open bars) and RVGect-G_8-Fib (filled bars).

(Fig. 5b). Again, very weak binding was observed with RVGect in comparison with RVGect-G_8-Fib, when the supernatants were not diluted. Furthermore, when recombinant RVGs were diluted a significant interaction with $p75^{NTR}$ could only be detected in the case of RVGect-G_8-Fib. This suggests that, although equivalent amounts of each recombinant RVG were used for cell staining, the proportion of active RVG may not be equivalent in the different samples. To test this hypothesis, we determined *in vitro* the concentration of active recombinant RVG, i.e. which is able to bind $p75^{NTR}$. We resorted to a method allowing us to determine the active concentration, by studying the change of binding rate to immobilized $p75^{NTR}$ with varying flow in partial mass transport conditions, which was developed for the Biacore surface plasmon resonance biosensor (Richalet-Secordel *et al.*, 1997). The results obtained showed that, in 20 times diluted supernatants, the active concentration of RVGect-G_8-Fib was two times higher than that of RVGect ($9{\cdot}0 \pm 1{\cdot}3$ against $4{\cdot}5 \pm 0{\cdot}9$ nM), although the expressed amount of RVGect-G_8-Fib was three to five times lower than that of RVGect (see results above). The proportion of active RVGect-G_8-Fib molecules is therefore six to 10 times higher than that of RVGect, at this dilution. Furthermore, we observed that the proportion of active RVGect molecules significantly diminished when the supernatant was further diluted, while that of RVGect-G_8-Fib remained virtually unchanged.

Altogether, these results indicate that RVG trimerization, induced by the fibritin foldon, is important to achieve an active conformation recognizing membrane-anchored and soluble $p75^{NTR}$.

Trimeric recombinant RVG and native RVG have similar $p75^{NTR}$ binding properties

We then performed a series of surface plasmon resonance assays to determine the kinetic parameters of the interaction between immobilized $p75^{NTR}$–His_6 and RVGect-G_8-Fib (Fig. 6). For RVGect supernatants, the concentration-dependent proportion of active trimeric molecules made it possible to acquire data only down to a 30-fold dilution and rendered the determination of the association

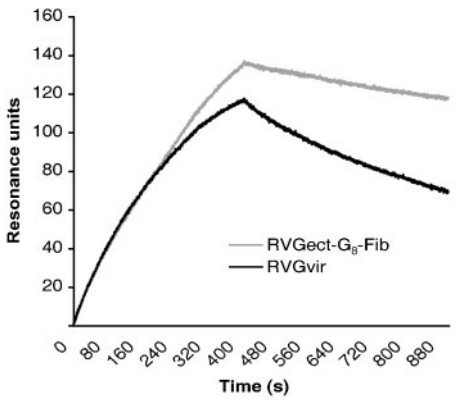

Fig. 6. Surface plasmon resonance real-time measurement of the interaction between RVG and immobilized $p75^{NTR}$–His_6. Representative sensorgrams are shown for RVGvir (6·2 nM) and RVGect-G_8-Fib (3·6 nM).

rate constant k_{on} impossible. On the contrary, for RVGect-G_8-Fib, signals significantly higher than the baseline noise were obtained even for 150-fold dilution of the supernatants, and the association (k_{on}) and dissociation (k_{off}) rate constants that we measured were concentration-independent and could be compared with the kinetic parameters obtained for the interaction between RVGvir and p75^{NTR} (Table 1). The k_{off} values for RVGect-G_8-Fib and RVGvir were virtually identical, and the k_{on} values were only twofold apart. The equilibrium dissociation constants (K'_d) for both molecules were therefore very close, in the low nanomolar range. Altogether, these results indicate that both recombinant RVG trimerized through the fibritin foldon and native RVG recognize p75^{NTR} in a very similar fashion.

DISCUSSION

In this work, we investigated the oligomerization state and functional characteristics of soluble recombinant RVG ectodomains, and demonstrated that the trimerization of RVG is necessary to enable efficient binding to the receptor p75^{NTR}.

We found that the fusion, at the C terminus, of a trimerization motif (the 27 aa foldon from the T4 bacteriophage fibritin), stabilized RVG's oligomeric structure. While RVGect formed unstable trimers that dissociated upon dilution, the chimeric recombinant RVGs (RVGect-Fib and RVGect-G_8-Fib) formed stable trimers. As for RVGect-Fib and RVGect-G_8-Fib, they sedimented in fractions 7, 8 and 9, close to the native trimeric RVG (RVGvir), which was found in fractions 6, 7 and 8 (Fig. 2). The difference could be explained by the relative size of the molecules (Fig. 1c): the recombinant chimeric RVG is 50 aa shorter than the viral RVG, and the sugar chains of glycoproteins expressed in insect cells are less complex than when mammalian cell expression systems are used (Jarvis & Finn, 1995).

Table 1. Kinetic parameters of the interactions between immobilized p75^{NTR} and soluble RVG

The determination of k_{on}, k_{off} and K'_d from Biacore experimental data are described in Methods. The mean value and associated standard error of three or more independent determinations are given.

RVG species	k_{on} (10^5 M^{-1} s^{-1})	k_{off} (10^{-4} s^{-1})	K'_d* (nM)
RVGvir	1·4±0·3	6·6±2·0	4·8±1·8
RVGect-G_8-Fib	2·7±0·4	5·2±2·0	1·9±0·8

*$K'_d = k_{off}/k_{on}$ is the equilibrium dissociation constant measured at the heterogeneous interface between the liquid phase and the sensorchip surface. There is no simple relation between this constant and the K_d that would be measured in a homogeneous solution.

Our data also constitute further evidence of the ability of the fibritin foldon to promote efficient trimerization of exogenous molecules (Miroshnikov *et al.*, 1998). Several studies have been performed with the adenovirus fibre, in which the fibritin foldon was shown to substitute efficiently the head of the molecule at the C terminus and to induce native-like trimerization of the whole fibre shaft (Krasnykh *et al.*, 2001) or its subdomains (Papanikolopoulou *et al.*, 2004a). In agreement with this observation, the structure of a chimeric molecule containing part of the adenovirus fibre fused to the fibritin foldon has recently been solved, showing that the structure of both components is identical to their counterpart in the native proteins (Papanikolopoulou *et al.*, 2004b). As previously reported in other studies (Papanikolopoulou *et al.*, 2004a), we observed that the presence of a linker between the RVG ectodomain and the foldon seems to further increase the stability of the trimer (Fig. 3a).

Staining of p75^{NTR}-expressing cells (Fig. 5) and surface plasmon resonance analysis showed that the proportion of active RVGect molecules (i.e. able to bind to p75^{NTR}) was concentration-dependent and decreased when the samples were diluted. On the contrary, the proportion of active RVGect-G_8-Fib molecules appeared to be concentration-independent. In agreement with these results, no staining of p75^{NTR}-expressing cells was observed when monomeric RVGect from fractions 10 and 11 of a sucrose gradient was used, while specific staining was detected using the same amount of trimeric recombinant RVGect-G_8-Fib from fractions 8 and 9 (data not shown). Therefore, our results demonstrate that the oligomerization state of RVG is crucial for its interaction with p75^{NTR}. Similar situations had previously been reported for TNF ligands (see Introduction), as well as for the interaction between the adenovirus fibre knob and its receptor (CAR), which involves a trimeric receptor–ligand avidity mechanism (Lortat-Jacob *et al.*, 2001). On the contrary, in the case of the respiratory syncitial virus, the interaction with cell surface proteoglycans is not dependent on the oligomerization state of the viral glycoprotein (Escribano-Romero *et al.*, 2004).

Our results finally demonstrate that the geometry of RVG trimerization is identical, whether it involves the C-terminal part of the RVG ectodomain and the transmembrane domain (RVGvir), or whether it is induced by the fibritin foldon (RVGect-G_8-Fib). Indeed, recombinant RVGect-G_8-Fib and native RVGvir interact with p75^{NTR} with very similar affinities and kinetic parameters (Table 1). However, the K'_d measured in this study with the Biacore for either RVGvir or RVGect-G_8-Fib is higher than that previously reported for the interaction between RVG and p75^{NTR} (2 nM against 30 pM) (Langevin *et al.*, 2002). This difference may be due to the fact that, in the previous report, RVG was organized in rosettes containing 8–10 trimers (Gaudin *et al.*, 1992), resulting in a significantly increased apparent avidity of RVG for p75^{NTR}.

Interestingly, the fibritin foldon not only appears to stabilize

the oligomeric structure of RVG and to preserve the functional properties of the binding site of $p75^{NTR}$, but it also maintains most of the antigenic structure of the native RVG (Fig. 4). Very few anti-RVG mAbs recognize RVGect; these results are in agreement with previously published reports, in which we have shown that soluble recombinant RVG ectodomain is antigenically distinct from native RVG (Gaudin *et al.*, 1999; Maillard & Gaudin, 2002). In contrast, RVGect-G_8-Fib was recognized by all the available mAbs, with the exception of those which are specific for site II, a conformational epitope consisting of aa 34–44 and 198–203. Therefore, in RVGect-G_8-Fib, although part of the N terminus of RVG is probably not in a strictly native conformation, its C terminus containing site III (a conformational site located between aa 330 and 340) and site 'a' (aa 342–343) seems to adopt a structure virtually identical to the native one. Interestingly, a site III- and trimer-specific antibody (Jallet *et al.*, 1999) interacts efficiently with the chimeric RVGect-G_8-Fib but not with RVGect. It is worth noting that amino acids that have been shown to be important for the interaction with $p75^{NTR}$ (residues 318 and 352) are also located in the carboxy part of RVG, on both sides of antigenic site III and site 'a' (Langevin & Tuffereau, 2002).

We can therefore propose a schematic representation of the native and recombinant RVGs (Fig. 7), illustrating their respective properties. In native RVGvir, the trimerization of the ectodomain is maintained both by its proximal C terminus and by the lipid-anchored transmembrane domain (Gaudin *et al.*, 1992; Maillard & Gaudin, 2002); RVGvir displays functional antigenic sites II, III and site 'a', and interacts with $p75^{NTR}$. In recombinant RVGect-G_8-Fib, stable trimeric oligomerization, required for interaction with $p75^{NTR}$, is promoted by the fibritin foldon at the carboxy end of the RVG ectodomain (aa 439). However, only antigenic sites 'a' and III have a fully native structure in these constructs. Lastly, recombinant RVGect forms unstable trimers (through the weakly associated C-terminal end of the ectodomain), which dissociate into monomers that display a non-native antigenic structure and do not interact with $p75^{NTR}$. In conclusion, C-terminal fusion of the RVG ectodomain with the fibritin foldon provides an efficient way to maintain a native-like conformation of a functionally crucial region of the molecule (from aa 300–439) involved in the interaction with $p75^{NTR}$. Experiments are currently in progress to determine whether trimeric RVG subdomains could be sufficient for the interaction with $p75^{NTR}$.

In conclusion, we have shown in this study that the trimerization of RVG is an important prerequisite for its interaction with $p75^{NTR}$, and we have identified an efficient method to promote stable trimerization of recombinant RVG through the fusion with the foldon domain of the phage T4 fibritin. This foldon also stabilizes the antigenic structure of the carboxy part of RVG; hence, the recombinant trimeric RVG could be a more potent immunogen than monomeric RVG. As a whole, our work opens up promising avenues

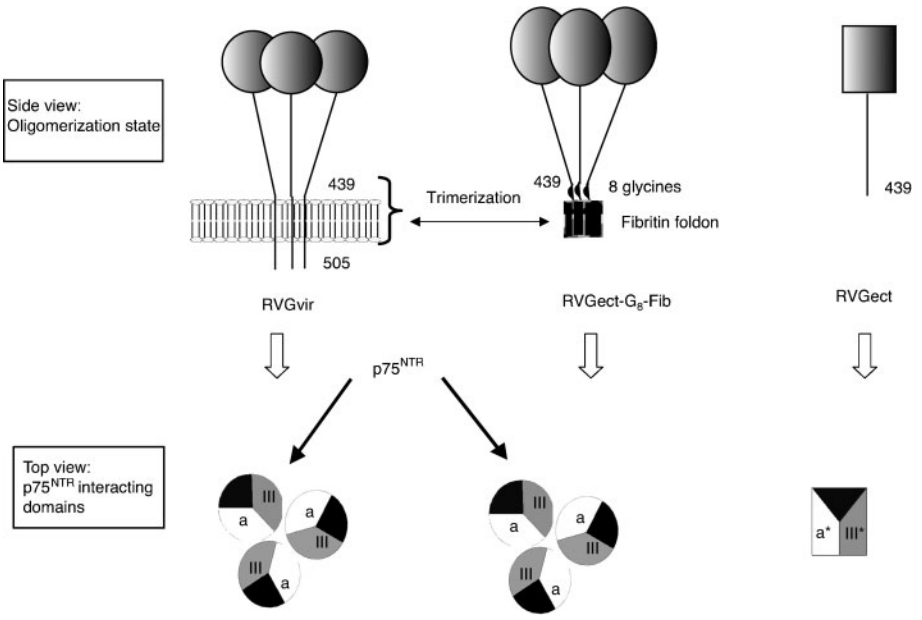

Fig. 7. Schematic representation of the different RVGs in relation to their $p75^{NTR}$ binding properties. In native RVGvir, stable trimeric association (side view) is maintained by its hydrophobic transmembrane domain and its proximal C-terminal domain, while in RVGect-G_8-Fib it is induced by the fibritin foldon. RVGvir and RVGect-G_8-Fib are both able to bind to $p75^{NTR}$ (top view) and they display similar antigenic structure in their C-terminal region. Grey, antigenic site III; white, site 'a'; black, the rest of the molecule (including site II). RVGect forms unstable trimers that dissociate into monomers, which are antigenically distinct from native RVG (Gaudin *et al.*, 1992) and are not able to bind to $p75^{NTR}$.

towards the determination of the structure of the p75^{NTR}–RVG complex, the precise characterization of the interaction domains that are involved and the investigation of the physiological effects mediated by RVG, a specific p75^{NTR} trimeric ligand.

ACKNOWLEDGEMENTS

The excellent technical assistance of Jacqueline Bénéjean is gratefully appreciated. We also thank Dr Letarov (SN Winogradsky Institute of Microbiology, Moscow, Russia) and Dr Mezyanzhinov (Institute of Bioorganic Chemistry, Moscow, Russia) for the gift of plasmid containing the T4 bacteriophage fibritin gene and anti-fibritin antibodies, respectively. This work was supported by CNRS funding and by research Grant QLRT-1999-00573 from the Fifth Framework Programme of the European Union. L. S. is the recipient of a doctoral fellowship from the Ministère de l'Education Nationale et de l'Enseignement Supérieur.

REFERENCES

Baldwin, A. N. & Shooter, E. M. (1995). Zone mapping of the binding domain of the rat low affinity nerve growth factor receptor by the introduction of novel *N*-glycosylation sites. *J Biol Chem* **270**, 4594–4602.

Benmansour, A., Leblois, H., Coulon, P., Tuffereau, C., Gaudin, Y., Flamand, A. & Lafay, F. (1991). Antigenicity of rabies virus glycoprotein. *J Virol* **65**, 4198–4203.

Cox, J. H., Dietzschold, B. & Schneider, L. G. (1977). Rabies virus glycoprotein. II. Biological and serological characterization. *Infect Immun* **16**, 754–759.

Desmezieres, E., Maillard, A. P., Gaudin, Y., Tordo, N. & Perrin, P. (2003). Differential stability and fusion activity of lyssavirus glycoprotein trimers. *Virus Res* **91**, 181–187.

Dietzschold, B., Gore, M., Marchadier, D. & 7 other authors (1990). Structural and immunological characterization of a linear virus-neutralizing epitope of the rabies virus glycoprotein and its possible use in a synthetic vaccine. *J Virol* **64**, 3804–3809.

Escribano-Romero, E., Rawling, J., Garcia-Barreno, B. & Melero, J. A. (2004). The soluble form of human respiratory syncytial virus attachment protein differs from the membrane-bound form in its oligomeric state but is still capable of binding to cell surface proteoglycans. *J Virol* **78**, 3524–3532.

Gaudin, Y., Ruigrok, R. W., Tuffereau, C., Knossow, M. & Flamand, A. (1992). Rabies virus glycoprotein is a trimer. *Virology* **187**, 627–632.

Gaudin, Y., Moreira, S., Benejean, J., Blondel, D., Flamand, A. & Tuffereau, C. (1999). Soluble ectodomain of rabies virus glycoprotein expressed in eukaryotic cells folds in a monomeric conformation that is antigenically distinct from the native state of the complete, membrane-anchored glycoprotein. *J Gen Virol* **80**, 1647–1656.

Harbury, P. B., Zhang, T., Kim, P. S. & Alber, T. (1993). A switch between two-, three-, and four-stranded coiled coils in GCN4 leucine zipper mutants. *Science* **262**, 1401–1407.

He, X. L. & Garcia, K. C. (2004). Structure of nerve growth factor complexed with the shared neurotrophin receptor p75. *Science* **304**, 870–875.

Hoppe, H. J., Barlow, P. N. & Reid, K. B. (1994). A parallel three stranded alpha-helical bundle at the nucleation site of collagen triple-helix formation. *FEBS Lett* **344**, 191–195.

Jallet, C., Jacob, Y., Bahloul, C., Drings, A., Desmezieres, E., Tordo, N. & Perrin, P. (1999). Chimeric lyssavirus glycoproteins with increased immunological potential. *J Virol* **73**, 225–233.

Jarvis, D. L. & Finn, E. E. (1995). Biochemical analysis of the *N*-glycosylation pathway in baculovirus-infected lepidopteran insect cells. *Virology* **212**, 500–511.

Kim, M. H., Billiar, T. R. & Seol, D. W. (2004). The secretable form of trimeric TRAIL, a potent inducer of apoptosis. *Biochem Biophys Res Commun* **321**, 930–935.

Krasnykh, V., Belousova, N., Korokhov, N., Mikheeva, G. & Curiel, D. T. (2001). Genetic targeting of an adenovirus vector via replacement of the fiber protein with the phage T4 fibritin. *J Virol* **75**, 4176–4183.

Lafay, F., Benmansour, A., Chebli, K. & Flamand, A. (1996). Immunodominant epitopes defined by a yeast-expressed library of random fragments of the rabies virus glycoprotein map outside major antigenic sites. *J Gen Virol* **77**, 339–346.

Lafon, M., Wiktor, T. J. & Macfarlan, R. I. (1983). Antigenic sites on the CVS rabies virus glycoprotein: analysis with monoclonal antibodies. *J Gen Virol* **64**, 843–851.

Langevin, C. & Tuffereau, C. (2002). Mutations conferring resistance to neutralization by a soluble form of the neurotrophin receptor (p75NTR) map outside of the known antigenic sites of the rabies virus glycoprotein. *J Virol* **76**, 10756–10765.

Langevin, C., Jaaro, H., Bressanelli, S., Fainzilber, M. & Tuffereau, C. (2002). Rabies virus glycoprotein (RVG) is a trimeric ligand for the N-terminal cysteine-rich domain of the mammalian p75 neurotrophin receptor. *J Biol Chem* **277**, 37655–37662.

Lentz, T. L., Burrage, T. G., Smith, A. L. & Tignor, G. H. (1983). The acetylcholine receptor as a cellular receptor for rabies virus. *Yale J Biol Med* **56**, 315–322.

Letarov, A. V., Londer, Y. Y., Boudko, S. P. & Mesyanzhinov, V. V. (1999). The carboxy-terminal domain initiates trimerization of bacteriophage T4 fibritin. *Biochemistry* **64**, 817–823.

Liepinsh, E., Ilag, L. L., Otting, G. & Ibanez, C. F. (1997). NMR structure of the death domain of the p75 neurotrophin receptor. *EMBO J* **16**, 4999–5005.

Locksley, R. M., Killeen, N. & Lenardo, M. J. (2001). The TNF and TNF receptor superfamilies: integrating mammalian biology. *Cell* **104**, 487–501.

Lortat-Jacob, H., Chouin, E., Cusack, S. & van Raaij, M. J. (2001). Kinetic analysis of adenovirus fiber binding to its receptor reveals an avidity mechanism for trimeric receptor-ligand interactions. *J Biol Chem* **276**, 9009–9015.

Maillard, A. P. & Gaudin, Y. (2002). Rabies virus glycoprotein can fold in two alternative, antigenically distinct conformations depending on membrane-anchor type. *J Gen Virol* **83**, 1465–1476.

McAlinden, A., Smith, T. A., Sandell, L. J., Ficheux, D., Parry, D. A. & Hulmes, D. J. (2003). Alpha-helical coiled-coil oligomerization domains are almost ubiquitous in the collagen superfamily. *J Biol Chem* **278**, 42200–42207.

McDonald, N. Q., Lapatto, R., Murray-Rust, J., Gunning, J., Wlodawer, A. & Blundell, T. L. (1991). New protein fold revealed by a 2·3-Å resolution crystal structure of nerve growth factor. *Nature* **354**, 411–414.

Miroshnikov, K. A., Marusich, E. I., Cerritelli, M. E., Cheng, N., Hyde, C. C., Steven, A. C. & Mesyanzhinov, V. V. (1998). Engineering trimeric fibrous proteins based on bacteriophage T4 adhesins. *Protein Eng* **11**, 329–332.

Mitraki, A., Barge, A., Chroboczek, J., Andrieu, J. P., Gagnon, J. & Ruigrok, R. W. (1999). Unfolding studies of human adenovirus type 2 fibre trimers. Evidence for a stable domain. *Eur J Biochem* **264**, 599–606.

Papanikolopoulou, K., Forge, V., Goeltz, P. & Mitraki, A. (2004a). Formation of highly stable chimeric trimers by fusion of an adenovirus fiber shaft fragment with the foldon domain of bacteriophage T4 fibritin. *J Biol Chem* **279**, 8991–8998.

Papanikolopoulou, K., Teixeira, S., Belrhali, H., Forsyth, V. T., Mitraki, A. & van Raaij, M. J. (2004b). Adenovirus fibre shaft sequences fold into the native triple beta-spiral fold when N-terminally fused to the bacteriophage T4 fibritin foldon trimerisation motif. *J Mol Biol* **342**, 219–227.

Park, Y. C., Burkitt, V., Villa, A. R., Tong, L. & Wu, H. (1999). Structural basis for self-association and receptor recognition of human TRAF2. *Nature* **398**, 533–538.

Prehaud, C., Coulon, P., LaFay, F., Thiers, C. & Flamand, A. (1988). Antigenic site II of the rabies virus glycoprotein: structure and role in viral virulence. *J Virol* **62**, 1–7.

Raux, H., Coulon, P., Lafay, F. & Flamand, A. (1995). Monoclonal antibodies which recognize the acidic configuration of the rabies glycoprotein at the surface of the virion can be neutralizing. *Virology* **210**, 400–408.

Richalet-Secordel, P. M., Rauffer-Bruyere, N., Christensen, L. L., Ofenloch-Haehnle, B., Seidel, C. & Van Regenmortel, M. H. (1997). Concentration measurement of unpurified proteins using biosensor technology under conditions of partial mass transport limitation. *Anal Biochem* **249**, 165–173.

Seif, I., Coulon, P., Rollin, P. E. & Flamand, A. (1985). Rabies virulence: effect on pathogenicity and sequence characterization of rabies virus mutations affecting antigenic site III of the glycoprotein. *J Virol* **53**, 926–934.

Shiraishi, T., Suzuyama, K., Okamoto, H. & 9 other authors (2004). Increased cytotoxicity of soluble Fas ligand by fusing isoleucine zipper motif. *Biochem Biophys Res Commun* **322**, 197–202.

Tao, Y., Strelkov, S. V., Mesyanzhinov, V. V. & Rossmann, M. G. (1997). Structure of bacteriophage T4 fibritin: a segmented coiled coil and the role of the C-terminal domain. *Structure* **5**, 789–798.

Thoulouze, M. I., Lafage, M., Schachner, M., Hartmann, U., Cremer, H. & Lafon, M. (1998). The neural cell adhesion molecule is a receptor for rabies virus. *J Virol* **72**, 7181–7190.

Tuffereau, C., Benejean, J., Alfonso, A. M., Flamand, A. & Fishman, M. C. (1998a). Neuronal cell surface molecules mediate specific binding to rabies virus glycoprotein expressed by a recombinant baculovirus on the surfaces of lepidopteran cells. *J Virol* **72**, 1085–1091.

Tuffereau, C., Benejean, J., Blondel, D., Kieffer, B. & Flamand, A. (1998b). Low-affinity nerve-growth factor receptor (P75NTR) can serve as a receptor for rabies virus. *EMBO J* **17**, 7250–7259.

Warrell, M. J. & Warrell, D. A. (2004). Rabies and other lyssavirus diseases. *Lancet* **363**, 959–969.

Welcher, A. A., Bitler, C. M., Radeke, M. J. & Shooter, E. M. (1991). Nerve growth factor binding domain of the nerve growth factor receptor. *Proc Natl Acad Sci U S A* **88**, 159–163.

Whitt, M. A., Buonocore, L., Prehaud, C. & Rose, J. K. (1991). Membrane fusion activity, oligomerization, and assembly of the rabies virus glycoprotein. *Virology* **185**, 681–688.

Wojczyk, B., Shakin-Eshleman, S. H., Doms, R. W., Xiang, Z. Q., Ertl, H. C., Wunner, W. H. & Spitalnik, S. L. (1995). Stable secretion of a soluble, oligomeric form of rabies virus glycoprotein: influence of *N*-glycan processing on secretion. *Biochemistry* **34**, 2599–2609.

Wojczyk, B. S., Stwora-Wojczyk, M., Shakin-Eshleman, S., Wunner, W. H. & Spitalnik, S. L. (1998). The role of site-specific N-glycosylation in secretion of soluble forms of rabies virus glycoprotein. *Glycobiology* **8**, 121–130.

Yan, H. & Chao, M. V. (1991). Disruption of cysteine-rich repeats of the p75 nerve growth factor receptor leads to loss of ligand binding. *J Biol Chem* **266**, 12099–12104.

Yang, X., Lee, J., Mahony, E. M., Kwong, P. D., Wyatt, R. & Sodroski, J. (2002). Highly stable trimers formed by human immunodeficiency virus type 1 envelope glycoproteins fused with the trimeric motif of T4 bacteriophage fibritin. *J Virol* **76**, 4634–4642.

Zeder-Lutz, G., Benito, A. & Van Regenmortel, M. H. (1999). Active concentration measurements of recombinant biomolecules using biosensor technology. *J Mol Recognit* **12**, 300–309.